Estimating groundwater contribution to transpiration using satellite-derived evapotranspiration estimates coupled with stable isotope analysis

S. Gokool[a,*], E.S. Riddell[a,b], A. Swemmer[c], J.B. Nippert[d], R. Raubenheimer[e], K.T. Chetty[a]

[a] School of Agriculture, Earth and Environmental Sciences, Centre for Water Resources Research, University of KwaZulu-Natal, Pietermaritzburg, South Africa
[b] Conservation Management, South African National Parks, Skukuza, South Africa
[c] South African Environmental Observation Network (SAEON), Ndlovu Node, Phalaborwa, South Africa
[d] Division of Biology, Kansas State University, Manhattan, KS, USA
[e] GCS Consulting, Pretoria, South Africa

ABSTRACT

The relative importance of groundwater (GW) to sustain terrestrial vegetation has been well documented. However, quantifying GW use by riparian vegetation in data scarce regions may prove to be challenging. For this purpose, we coupled evapotranspiration (ET) estimates from the satellite-based surface energy balance system (SEBS) model with stable isotope analysis, to map and quantify the contribution of GW to transpiration (ET_g), along the lower reaches of a perennial river system, in the semi-arid north-eastern region of South Africa. Plant stem, soil, stream and GW samples were collected on 3 sampling occasions during the 2016 dry season. δ^2H and δ^{18}O values of the respective samples were measured and analysed. We found that while GW use was prevalent and increased with aridity, overall ET_g was fairly minimal. During the initial stages of the dry season ET_g for the study area was extremely low, approximately 0.10% of daily ET or 0.01 mm d^{-1}. However, as aridity increased, ET_g increased to approximately 10% of daily ET or 0.30 mm d^{-1}. The results of these various investigations undertaken demonstrates the potential of coupling satellite-based ET approaches with stable isotope analysis, to quantify spatial and seasonal dynamics in ET_g.

1. Introduction

In arid and semi-arid environments groundwater (GW) is often the most important source of freshwater for human consumption, for vegetation and makes a significant contribution to streamflow (Lange, 2005). Therefore, balancing the amount of GW that is used for basic human needs with environmental water requirements (EWR) is crucial for successful water resource management in these regions (Tanner and Hughes, 2015). According to Eamus et al. (2015), quantifying seasonal and spatial variations GW consumption by vegetation is one of the key areas which can facilitate the sustainable management of GW resources, especially the EWR flow allocations of this resource.

In the last decade, ET estimation, has substantially benefited from advancements in satellite earth observation techniques (SEO) (Nourhi et al., 2013). SEO techniques can be used to quantify the water use of riparian vegetation and are often utilized to overcome spatial limitations generally associated with conventional approaches, such as *inter alia*; FAO 56 Penman Monteith reference evaporation, eddy covariance, scintillometry (Allen et al., 1998; Savage et al., 2004; Fernández-Prieto et al., 2012; Jassas et al., 2015). Furthermore, SEO can be used to

acquire data in remote and data scarce regions, as well as allowing for seasonal and inter-annual comparisons of hydro-meteorological variables due to the periodic updating of information (Gokool et al., 2017a).

Despite these advantages, the trade-off between the spatial and temporal resolution of available imagery and the ability of the models to accurately estimate fluxes and ET in different environmental settings, may limit the use of SEO technologies to guide water resources management decisions (Gokool et al., 2017a). While there exist approaches to address these limitations and improve upon the accuracy of ET estimates (Hong et al., 2011; Pardo et al., 2014; Gokool et al., 2017a), the ET estimate provided is often the total water used from multiple sources such as; soil water, GW or stream water. Therefore, the ET estimate acquired by these techniques requires further disaggregation to determine ET_g (Eamus et al., 2015).

Several studies have identified approaches to quantify subsurface moisture dynamics at varying spatial and temporal scales, because the movement of water in the soil-root system plays a significant role in regulating ecohydrological processes at the surface (Kumar et al., 2014; Daly et al., 2017). These techniques include; conventional approaches

---

(time-domain reflectometry, gravimetric methods and neutron probes), isotope hydrology, geophysical techniques (electrical resistivity imaging), the cosmic ray probe, SEO data and root water uptake models (Robinson et al., 2012; Villarreyes et al., 2013; Kumar et al., 2014; Mares et al., 2016; Daly et al., 2017; Zhang et al., 2017).

Isotope hydrology and in particular environmental isotopes (stable and radioactive) techniques are amongst the most effective and frequently used tools to understand and quantify soil-plant-water dynamics (Yang et al., 2010; Penna et al., 2013). While both radioactive and stable isotopes have been extensively applied for ecohydrological investigations (Marwick et al., 2015; Thaw et al., 2016; Zhang et al., 2017; Evaristo and McDonnell, 2017), the use of stable isotope techniques has generally been applied more frequently for quantifying the depth and sources of water uptake for transpiration (Penna et al., 2013; Thaw et al., 2016).

For most species and locations, the uptake of water during transpiration does not generally result in the fractionation of oxygen-18 (^{18}O) and deuterium (^{2}H) within non-photosynthesising tissue (Evaristo and McDonnell, 2017). The isotopic composition of ^{18}O and ^{2}H of xylem water should represent the sources present within the root zone (Evaristo and McDonnell, 2017). Although this assumption has been supported and well documented in various soil-plant-water interaction studies (Zimmermann et al., 1966; White et al., 1985; Walker and Richardson, 1991; Dawson et al., 2002), it should be noted that certain plant species within particular environmental settings may fractionate ^{2}H during root water uptake (see: Lin and da Sternberg, 1993; Ellsworth and Williams, 2007; Zhao et al., 2016; Evaristo et al., 2017).

In this study, we aimed to quantify ET_g along the riparian zone situated in the lower reaches of a perennial river system in the semi-arid north-eastern region of South Africa, employing a relatively simplistic approach that requires two independent types of data; (i) daily estimates of ET and (ii) the stable isotopic composition of ^{18}O and ^{2}H of xylem water and all possible sources.

Once the proportional contribution of these sources to the xylem water has been established, ET_g can be derived as the product of the GW proportion and ET (Eamus et al., 2015). Based on the aforementioned approach, we implemented the satellite-based Surface Energy Balance System (SEBS) Model and two approaches, to quantify daily ET at a moderate spatial resolution (MSR) (Gokool et al., 2017a).

ET estimates acquired from these approaches were evaluated against *in-situ* measurements of ET acquired from a one-sensor (excludes Infra-Red Gas Analyser) Eddy Covariance system (EC_{ET}), in order to determine which approach most adequately represents the ET for the portion of river reach studied. During a separate investigation, we coupled isotope analysis of ^{18}O and ^{2}H with a Bayesian mixing model to determine the proportional contribution of water sources to transpiration.

The results from these investigations were then used to provide insights on spatial and seasonal dynamics in ET_g within the study area. Furthermore, the timing of this study also coincided with a large El Nino induced drought period (Kogan and Guo, 2016), providing further insights into plant water use dynamics during extreme drought conditions.

2. Methodology

2.1. Study area

The study site is situated in the Limpopo Province in the north-eastern region of South Africa, along the lower reaches of the Groot Letaba River between Letaba Ranch (B8H007; 23.658° S; 31.047° E) and Mahale (B8H007; 23.669° S; 30.991° E) weirs, as depicted in Fig. 1. According to Pollard and du Toit (2011), the Letaba River system often experiences water shortages and restrictions and has frequently been unable to meet its EWR. Therefore, understanding and accurately quantifying the dynamics of vegetation water use requirements in this

region, is essential to maintain the natural functioning of this environment. A semi-arid climate, characterized by hot wet summers and mild dry winters is experienced across the region. Mean annual temperatures vary across the region ranging from 18 °C in the mountainous areas to 28 °C in the eastern regions (Katambara and Ndiritu, 2010).

A majority of the rainfall occurs in the summer months (October to March) and is predominantly characterized by thundershowers occurring from the north and north-east, as well as from tropical cyclones originating over the Indian Ocean (Katambara and Ndiritu, 2010; February et al., 2007). According to Heritage et al. (2001) approximately three quarters of the catchment is underlain by granite and gneiss. There exists a variety of morphological units within the study area which is due to the varied distribution of sediment along the river. The portion of the Groot Letaba River flowing through the study area is largely characterized by alluvial channel types (Heritage et al., 2001). The study area was categorized into three separate geomorphological zones during sampling. These were; i) the near stream northern and ii) southern banks which includes the alluvial terrace situated adjacent to the active stream channel, as well as iii) within the active river channel.

The total area of the river channel and riparian zone contributing to ET was estimated to be approximately 1.96 km². This was calculated by summing up the width of the river channel (approximately 60 m and constitutes 50% vegetation, 30% bare soil and 20% open water) and riparian zone (40 m on either side of the channel and complete vegetation coverage) and multiplying it by the longitudinal distance of the portion of river reach studied between the two weirs (14 000 m) (Gokool et al., 2017a; Riddell et al., 2017).

A variety of woody plant species were situated along geomorphological zones i and ii. The common species included; *Ficus sycomorus*, *Philonoptera violecia*, *Diospyros mespiliformis*, *Colophosphermum mopane*, *Combretum microphyllum*, *Gymnosporia senegalensis*, *Cassia abbreviata and Ziziphus mucronata*. While the predominant plant species situated within geomorphological zone iii is *Phragmites mauritianus*. Additionally, numerous agricultural fields, predominantly planted with *Cucurbita moschata* and *Medicago sativa* are situated further away from the active river channel. These were however not considered during sampling.

43 individual trees from the abovementioned species; 9 *F. sycomorus*, 8 *P. violecia*, 10 *D. mespiliformis*, 3 *C. mopane*, 3 *C. microphyllum*, 5 *G. senegalensis* and 5 *Z. mucronata* distributed among the six sampling regions, were randomly selected and sampled for subsequent stable isotope analysis (Lin et al., 2016). These sampling regions were categorized, according to their respective locations with regards to Letaba Farm (20 trees) and Letaba Ranch (26 trees). Fig. 1 provides a Google Earth™ illustration of the sampling regions distributed between the farming areas and Letaba Ranch.

2.2. Estimation of daily ET

SEBS was applied in this study to estimate daily ET. Su (2002) provides a detailed conceptualization of the model. However, the underlying principle of SEBS, is to compute all components of the shortened surface energy balance (Equation (1)), as well as the evaporative fraction (*EF*), using land surface parameters which are derived from meteorological and SEO sources, respectively (Su, 2002).

$$R_n = Go + H + \lambda E \tag{1}$$

Where *Rn* is net radiation (W m^{-2}), G_O is soil heat flux (W m^{-2}), *H* is sensible heat flux (W m^{-2}) and λE is the latent heat flux (W m^{-2}).

While the original SEBS formulation ($SEBS_O$) has been widely implemented and shown to be a credible approach for the estimation of regional fluxes and ET. Studies (Pardo et al., 2014; Gokool et al., 2017a) have shown, that the model may over-estimate the *EF* and subsequently the ET during conditions of water stress, as it is unable to adequately account for the influence of soil moisture availability and biophysical characteristics during the estimation of ET. Subsequently, a modified
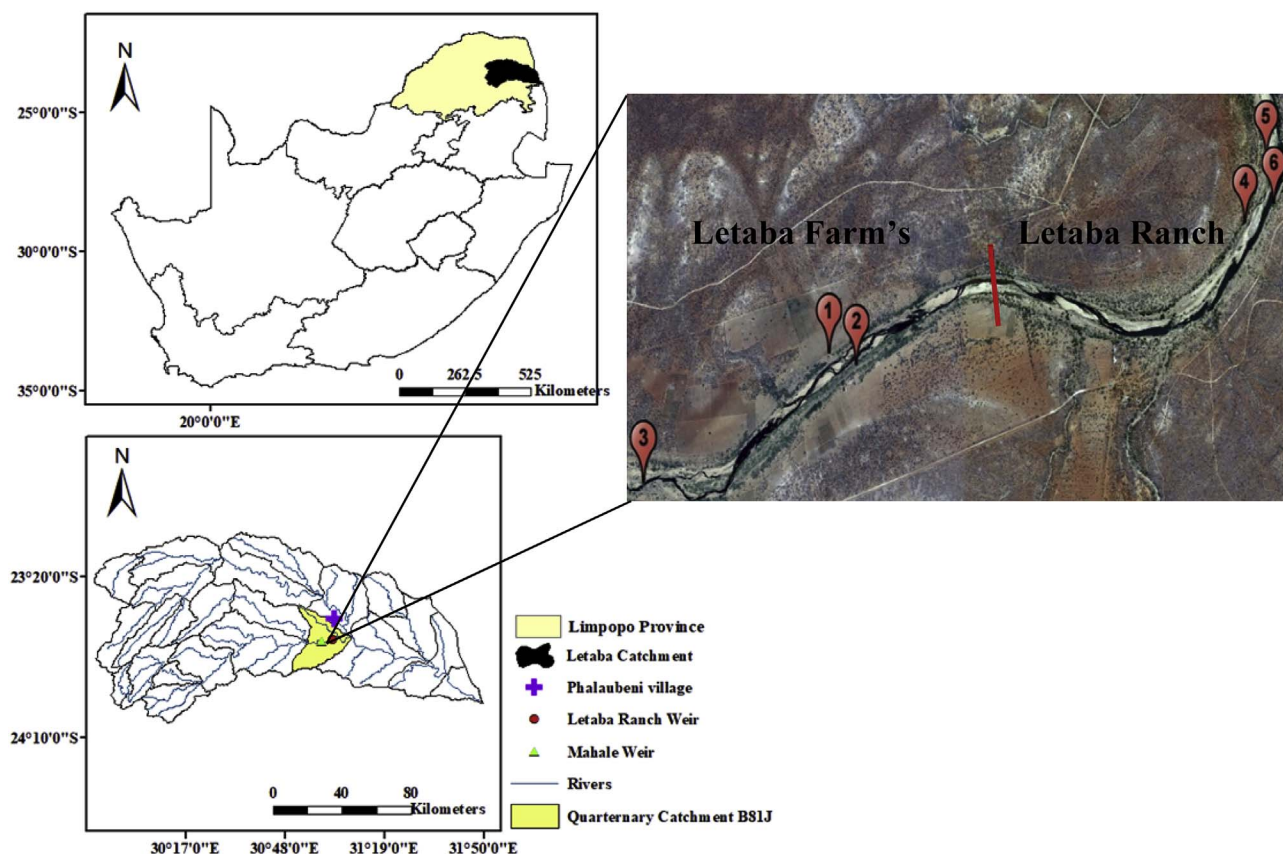
Fig. 1. Location of the study area and stable isotope sampling points (Google Earth ™ image), situated along the lower reach of the Groot Letaba River within the Quaternary catchment B81J (adapted from Schulze et al., 1997).

version of SEBS (*SEBS_ESF*), which was proposed as a means to improve upon ET estimation for water limited environments, was applied in this study. The *SEBS_ESF* approach detailed in Gokool (2017b) attempts to improve upon the estimation of the *EF* and daily ET, through the integration of a calibration factor in *SEBS_O*, so that the influence of environmental stress is more adequately represented during the estimation of ET.

Daily ET estimates were derived in *SEBS_ESF* using SEO data acquired from both Landsat and MODIS, as well as meteorological data measured *in situ* (Riddell et al., 2017). 215 clear sky MODIS Level 1 B Terra images (MOD21 and MOD 03 data products, available daily at a 1 km spatial resolution), as well as 26 clear sky Landsat (7 and 8) Level 1 GeoTiff images (available every 16 days at a 30 m spatial resolution) were acquired, during 2015 and 2016 (18th June to 31st October). Preprocessing and processing of these images were undertaken based on the procedures detailed in Su and Wang (2013), Singh et al. (2014) and USGS (2015).

Although the use of Landsat and MODIS data in SEBS facilitates the relatively timeous and inexpensive quantification of ET. The spatial and temporal resolutions associated with these data sets may limit their feasibility to estimate ET for operational water resources management (Gokool et al., 2017a). In order to, overcome these limitations; two techniques, a simple output downscaling with linear regression (ODLR) and the actual crop coefficient (*Kc_act*) approach as described in Gokool et al. (2017a) were applied and evaluated.

The daily ET estimates derived from implementing *SEBS_ESF* were used as inputs to these approaches to produce a time-series of daily ET at a MSR. The ODLR and *Kc_act* derived ET estimates were then evaluated through statistical comparisons with *EC_ET*. Only the values from satellite-pixels covering the location of the EC system were used during data comparisons. The results from these investigations were then used to determine which approach most adequately represents the riparian

ET within the study area. A detailed description of the instrumentation setup, study site and data collection for ET and meteorological variables is given in Gokool et al. (2017a) and Riddell et al. (2017).

2.3. Water sampling and isotope analyses

Plant stems, soil, stream and GW samples were collected on 3 sampling occasions during the 2016 dry season (in May, August and October) which are representative of the late autumn, late winter and mid spring seasons, respectively in the study area. During this period (from May to October) the study area usually experiences drier conditions and low flows, a critical period with regards to water shortages. From the 43 individual trees, stem samples of mature wood approximately 0.30–1.00 cm in diameter and 4.00–7.00 cm in length were collected. These samples were collected from randomized locations from each tree and the epidermis was removed immediately, before being transferred into small airtight glass vials (Lin et al., 2016). Soil samples at depths of 30, 60, 100 and 140 cm were collected concurrently with the twig samples. The soil samples were obtained using a hand auger and then transferred and sealed into airtight 500 ml plastic bottles.

Stream samples were collected at sampling points 1, 3 and 6 and stored in airtight 500 ml plastic bottles. Each sample bottle was rinsed three times with the sample water before the actual sample was taken. GW samples were collected from 5 boreholes situated adjacent to the active river channel at sampling points 1, 3, 4 and 5, as well as from a borehole situated within the active river channel at sampling point 6. The boreholes were purged, ensuring steady state chemical conditions (stable electrical conductivity and pH) were reached, so that a GW sample representative of the surrounding aquifer could be collected.

These samples were then stored in airtight 500 ml plastic bottles. In order to, ensure that an unevaporated sample was collected from the

Table 1
Statistical comparison of Kc_{act} and ODLR ET estimates derived from implementing $SEBS_0$ and $SEBS_{ESF}$, against EC_{ET} during the 2015 and 2016 period of investigation.

	Kc_{act} ET derived from $SEBS_0$	Kc_{act} ET derived from $SEBS_{ESF}$	ODLR ET derived from $SEBS_0$	ODLR ET derived from $SEBS_{ESF}$
RVE	−72.24	−5.82	−100.25	8.40
Bias	1.10	0.62	1.68	0.76
RMSE	1.35	0.87	2.03	1.04
Kruskal-Wallis (p value)	0.00	0.60	0.00	0.05
Correlation Coefficient	0.48	0.79	0.30	0.74
Nash-Sutcliffe	0.03	0.60	−1.21	0.42

borehole, the pump was left to run continuously while the representative sample was being collected (Riddell et al., 2016). The various samples collected in field were stored in a cooler bag and then stored in a fridge prior to transportation to the laboratory for analysis in the following days.

Rainfall data for the study area was collected from a Davis™ Vantage Pro2 station situated in Phalaubeni, approximately 6 km north of the study site. However, there were very few rain events experienced on site due to the drought. Subsequently only a limited number of samples were available for analysis. 10 rainfall samples from 15th November 2015 to 19th May 2016 were collected and analysed. The δ^2H and $\delta^{18}O$ values for these precipitation events were then used to construct a local meteoric water line (LMWL) for our study site. The δ^2H and $\delta^{18}O$ values for all our samples were then plotted and compared relative to this LMWL. ^2H and ^{18}O contents of rainfall, stream and GW samples were measured using a Los Gatos Research (LGR) DLT-100 Liquid Water Isotope Analyser.

Plant stem and soil waters were extracted using a 2-step cryogenic open manifold system that facilitated the removal of non-condensable gases and potential organic contaminants (Nippert and Knapp, 2007). This extraction procedure minimizes the likelihood of organic molecules influencing the isotopic signature of the water extracted from plants and soils. Furthermore, the "ChemCorrect" software offered by Picarro, was used to screen the samples post-analysis (West et al., 2011), to identify samples that should be excluded from further analysis.

^2H and ^{18}O contents of the xylem water and soil water were measured using a Picarro L1102-i CRDS analyser (Picarro, Santa Clara, California, USA). The overall analytical precision of both the spectrometers was less than 2 permil ($0.002‰$) for ^2H and less than 0.3 permil ($0.0003‰$) for ^{18}O.

The ^2H and ^{18}O of the various samples (^2H and ^{18}O) were expressed in delta notation relative to the Vienna Standard Mean Oceanic Water (VSMOW), as:

$$\delta = \left(\frac{R_{sample}}{R_{standard}} - 1 \right) * 1000 \qquad (2)$$

Where δ (expressed in $‰$ notation) represents changes in the ratio of the uncommon to common isotopes ($^2H/^1H$ and $^{18}O/^{16}O$) for the sample (R_{sample}) and standard ($R_{standard}$).

The freely available stable isotope mixing model package in R (Simmr), which has been designed to solve mixing equations for stable isotope data using a Bayesian statistical framework (Parnell and Inger, 2016), was used to identify proportional contributions of sources to transpiration. Bayesian mixing models such as Simmr possess several advantages over conventional linear mixing models, such as their ability to quantify; i) the proportional contribution of water sources to transpiration, ii) account for uncertainties associated with the sources and iii) allowing for the input of isotope data from multiple sources (Ma and Song, 2016).

The Simmr package requires three sets of input data as a minimum, to determine the proportions of water used from a particular source, this includes; i) δ^2H and $\delta^{18}O$ of the xylem water, ii) mean δ^2H and $\delta^{18}O$ for the various sources and iii) standard deviations of δ^2H and $\delta^{18}O$ for the various sources (Parnell and Inger, 2016). The isotopic composition of GW and stream water was found to be statistically different (non-parametric Mann-Whitney test p < 0.05). Similarly, soil δ^2H and $\delta^{18}O$ values at each of the depth regions that were sampled were found to be statistically different from each other (Mann-Whitney test p < 0.05). Subsequently, the potential sources of water used during transpiration were considered to be soil water (at each depth region sampled), GW and stream water (Penna et al., 2013; Phillips et al., 2014; Zhang et al., 2017).

Simmr was implemented with 100 000 iterations (discarding the first 10 000), no prior information was used to guide the model, thus all sources had an equal likelihood of contribution (Zhang et al., 2017). Trophic enrichment factors and concentration dependence values were set to zero.

The estimated proportions of source contribution to the xylem mixture were subsequently determined using a Markov Chain Monte Carlo function to repeatedly estimate the proportions of the various sources in the mixture and determine the values which best fit the mixture data (Parnell and Inger, 2016). The median (50% quantile) source contribution value determined for each of the sources was then used during analytical comparisons and subsequent investigations.

3. Results

3.1. Estimation of daily ET using satellite earth observation data

Statistical comparisons between the Kc_{act} and ODLR ET estimates against the EC_{ET} is presented in Table 1. The implementation of $SEBS_{ESF}$ resulted in an improved estimation of the daily ET derived at a MSR for both the Kc_{act} and ODLR approaches, as illustrated in Fig. 2. The correlation between modelled and observed ET, improved from 0.48 to 0.79 and 0.30 to 0.74, respectively for Kc_{act} and ODLR ET estimates. Furthermore, there was a significant increase in Nash-Sutcliffe efficiency values. While the use of $SEBS_{ESF}$ ET estimates as inputs to the Kc_{act} and ODLR approaches, resulted in an improved estimation of the daily ET at a MSR. The Kc_{act} approach was selected to quantify daily ET, due to the reduced bias and higher correlations achieved between the modelled and observed ET.

3.2. Isotopic composition of water

δ^2H in rainfall ranged from −22.9–15.30$‰$, with a mean value of 0.20$‰$ ($±11.60‰$). Whereas $\delta^{18}O$ in rainfall ranged from −4.30–0.90$‰$, with a mean value of −1.70$‰$ ($±1.60‰$). The LMWL for our study site, as shown in Fig. 3, was established as $\delta^2H = 7.06\delta^{18}O + 12.13$, with a R^2 value of 0.89. The slope of the LMWL is lower than the slope of the global meteoric water line, described respectively in Craig (1961) and Liu et al. (2014), as $\delta^2H = 8\delta^{18}O + 10$ and $\delta^2H = 7.94\delta^{18}O + 3.92$. This can be attributed to rapid evaporation of falling raindrops (Ma and Song, 2016), which would be expected in this semi-arid region. Due to the limited number of rainfall samples collected, the LMWL that was generated may not be representative of the conditions experienced during the collection of the other isotope samples.

Subsequently, we also plotted the Pretoria meteoric water line described in Mekiso et al. (2015), as $\delta^2H = 7.05\delta^{18}O + 7.60$ (Fig. 3), for a site approximately 400 km away and based on a far longer time series, so that any regional climatic differences in the rainfall received within our study site could also be determined. Rainfall during the study period was generally dominated by convective rainfall with lighter isotopes, the exception being the rain during March and a single event in May 2016 which had a much more depleted signature.
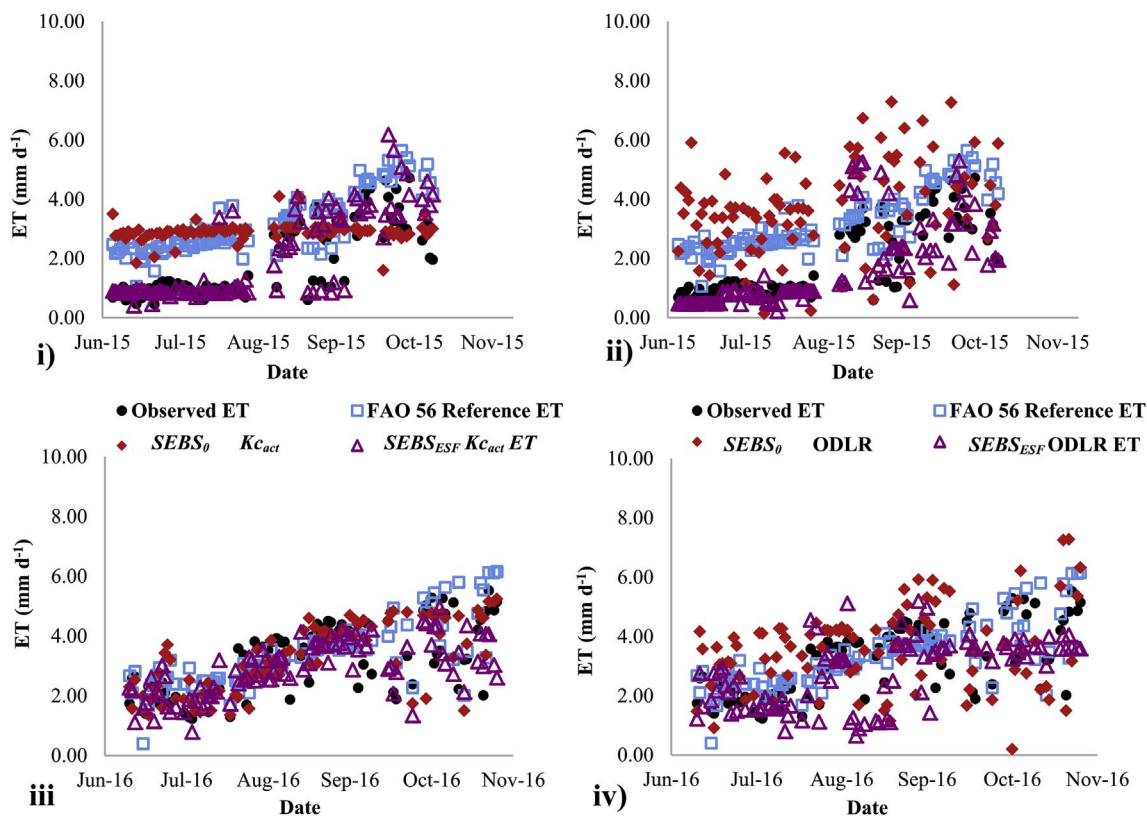
Fig. 2. A comparison of observed and modelled ET derived using the *Kc_act* and ODLR approaches during the 2015 (i and ii) and 2016 (iii and iv) period of investigation.

The δ^2H and $\delta^{18}O$ of stream water, soil water and xylem water plot below the LMWL, showing evaporative enrichment in these samples relative to rainfall, as shown in Fig. 4 δ^2H and $\delta^{18}O$ values for GW plot closest to the LMWL providing evidence that precipitation is one of the principal sources to GW. δ^2H in surface water ranged from −9.16–9.48‰, with a mean value of −1.32‰ (± 6.78‰). Whereas $\delta^{18}O$ in surface water ranged from −1.85–2.75‰, with a mean value of 0.19 (± 1.79‰).

δ^2H in soil water (30, 60, 100 and 140 cm) ranged from −53.00–7.00‰, with a mean value of −23.95‰ (± 14.89‰). Whereas $\delta^{18}O$ in soil water (30, 60, 100 and 140 cm) ranged from −6.90–7.90‰, with a mean value of −1.06 (± 3.25‰). δ^2H and $\delta^{18}O$ in soil water were enriched in the top soil layers and generally depleted with depth. The higher levels of enrichment associated with the δ^2H and $\delta^{18}O$ values of soil water in the upper soil layers are due to the effects of

evaporation at the surface.

This observation is reaffirmed by the lower slope of the fitting line of the soil water δ^2H and $\delta^{18}O$ (SEL) relationship in comparison to the LMWL (Fig. 4), being indicative of the strong evaporation effect on soil moisture which is characteristically associated with semi-arid regions. The higher levels of depletion generally associated with soil water deeper down the profile could presumably be attributed to deep pre-ferential infiltration of heavy rainfall events.

δ^2H in xylem water ranged from −65.00–6.00‰, with a mean value of −29.56‰ (± 19.65‰). Whereas $\delta^{18}O$ in xylem water ranged from −8.00–6.20‰, with a mean value of −2.63(± 3.19‰). The isotopic composition of δ^2H and $\delta^{18}O$ in the xylem water were shown to gen-erally plot closest to the SEL (Fig. 5), indicating that soil water is one of the main contributors to ET.

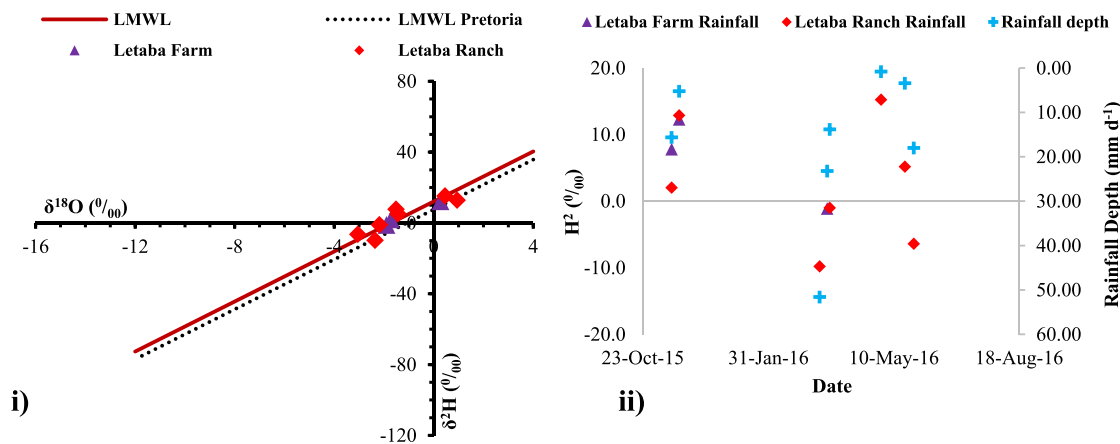δ^2H and $\delta^{18}O$ values of xylem water were generally concentrated

Fig. 3. i) Stable isotopes of rainfall during the study period against LMWL and ii) time-series comparison.
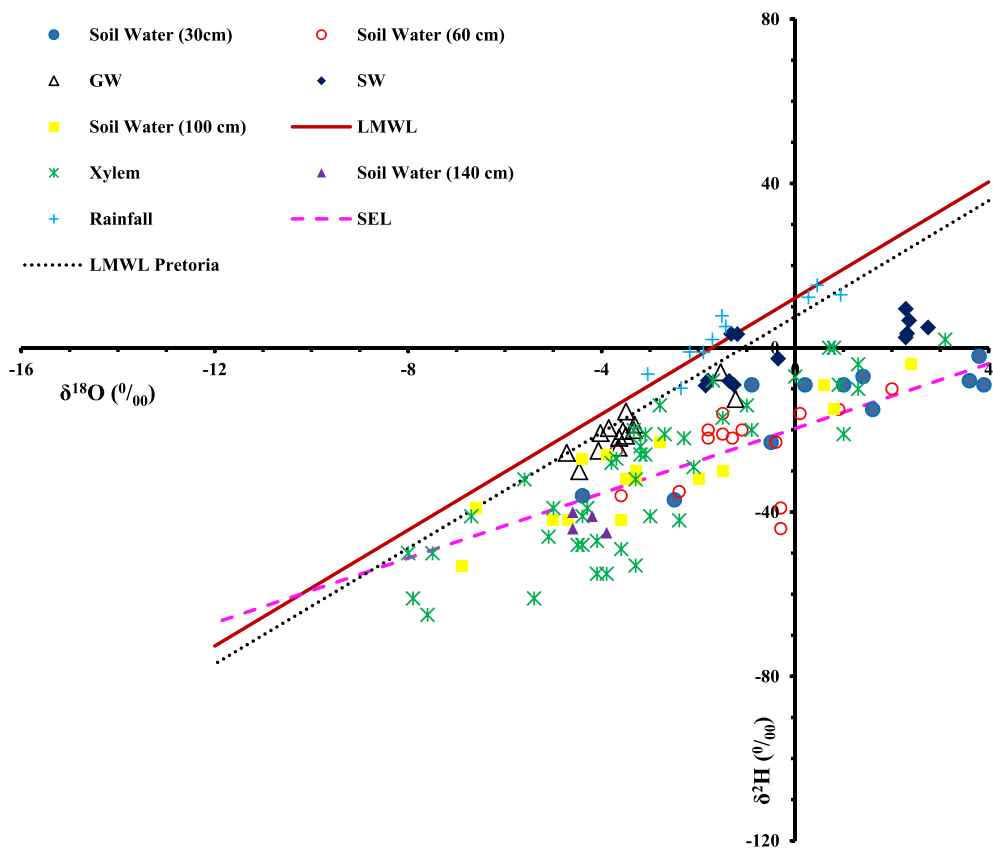
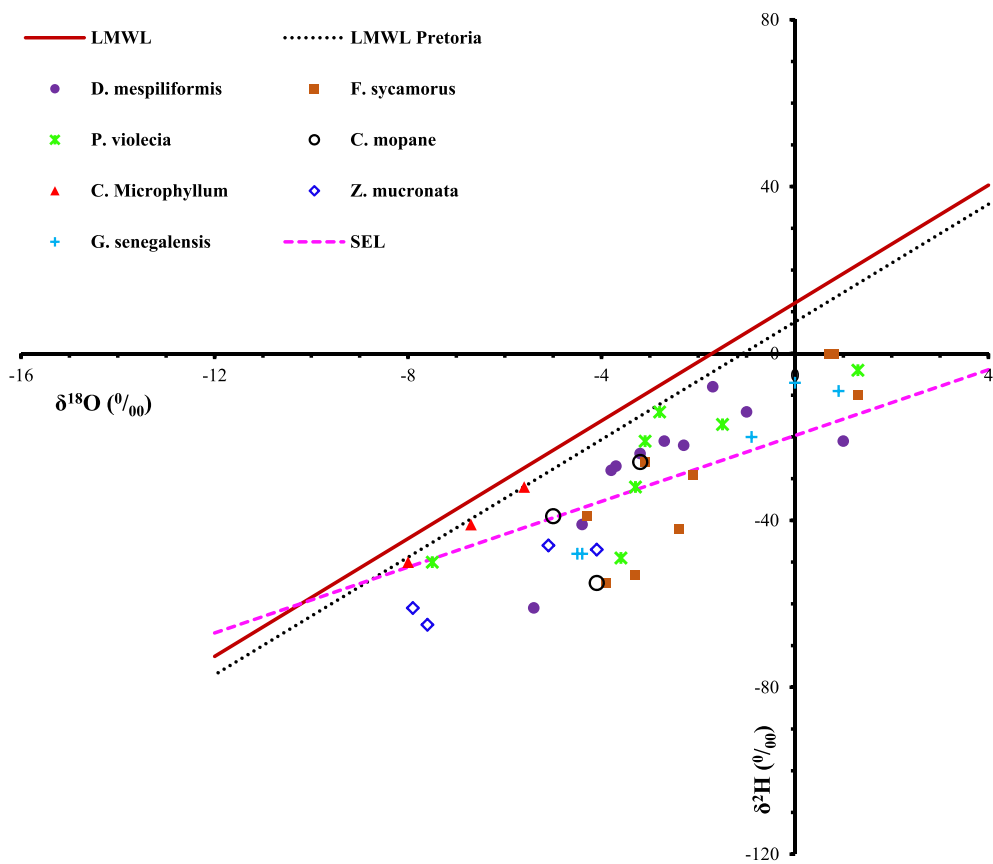**Fig. 4.** A plot of the relationship between δ^2H and $\delta^{18}O$ values for all water samples.

Fig. 5. A plot of the relationship between δ^2H and $\delta^{18}O$ values for individual plant species.

Table 2
Average proportional contribution of sources to individual plant species for the three sampling campaigns.

Tree species	Ground water	Surface water	Soil water (30 cm)	Soil water (60 cm)	Soil water (100 cm)	Soil water (140 cm)
F. sycamorus	1.50%	1.70%	1.60%	1.70%	72.40%	20.20%
P. violecia	4.40%	3.50%	4.90%	5.60%	73.60%	5.40%
D. mespiliformis	2.30%	2.90%	2.60%	2.80%	70.00%	17.50%
C. mopane	1.10%	0.70%	1.50%	2.00%	3.80%	89.50%
C. Microphyllum	1.20%	0.90%	1.50%	1.90%	16.10%	77.50%
G. senegalensis	1.50%	1.70%	1.60%	1.80%	67.00%	25.40%
Z. mucronata	1.10%	0.60%	1.50%	2.00%	3.30%	90.00%

around an uptake depth between 60 and 140 cm. This observation is reaffirmed by the results of the proportional contributions of sources to ET, shown in Table 2.

4. Discussion

It has been shown that the water uptake patterns vary considerably amongst the trees that were sampled. However, these results could not be combined with the satellite-derived ET estimates to determine seasonal variations in ET_g for each plant species due to the mixed-pixel effect (Gibson et al., 2011). Due to this limitation, seasonal variations in ET_g at each location, as well as for the entire study area were quantified instead. Location specific δ^2H and δ^{18}O values of xylem and source waters were used as inputs to a mixing model (Simmr) to determine the proportional contribution of GW to ET during each month (Table 3). ET_g was then determined as the product of these values and the average daily ET for each month, as shown in Fig. 6.

During the three sampling campaigns soil water was found to be the major contributing source to ET at each sampling location (approximately 88%). Whereas GW contribution to ET was relatively low ranging from 0.20 to 10.00%. The average daily ET_g during these periods ranged from 0.00 to 0.38 mm d^{-1}, with a mean value of 0.12 mm d^{-1}. Whereas average daily ET along the river reach ranged from 1.78 to 3.70 mm d^{-1}, with a mean value of 2.89 mm d^{-1}. Although GW contribution to ET was fairly low, it is evident that there are seasonal changes in water uptake patterns at each sampling location.

This occurrence can be largely attributed to the antecedent moisture

Table 3
Proportional contribution of sources to ET during the three sampling campaigns.

	Location	Ground water	Surface water	Soil water (30 cm)	Soil water (60 cm)	Soil water (100 cm)	Soil water (140 cm)
May	1	1.40%	1.00%	2.00%	1.00%	1.20%	89.00%
	2	0.40%	17.50%	0.40%	0.40%	80.80%	0.30%
	3	0.20%	0.10%	0.60%	1.20%	0.10%	97.00%
	4	0.80%	41.00%	0.80%	0.90%	54.60%	1.70%
	5	1.30%	1.70%	1.40%	1.50%	56.70%	36.40%
	6	2.10%	0.70%	10.80%	22.20%	62.40%	1.10%
Aug	1	8.30%	8.50%	43.00%	6.20%	22.70%	8.50%
	2	10.20%	6.00%	11.30%	25.00%	17.00%	26.00%
	3	2.00%	3.00%	1.60%	1.80%	6.20%	85.00%
	4	6.00%	3.00%	14.00%	30.00%	42.00%	3.40%
	5	0.50%	0.50%	0.50%	0.70%	67.10%	30.40%
	6	6.10%	1.50%	32.60%	53.90%	2.90%	1.90%
Oct	1	6.10%	4.00%	8.00%	7.40%	9.00%	61.00%
	2	4.20%	2.20%	5.00%	6.00%	4.00%	76.00%
	3	0.90%	1.20%	0.90%	0.10%	43.00%	53.00%
	4	7.00%	14.00%	6.10%	6.10%	8.00%	56.00%
	5	0.30%	0.20%	0.40%	0.40%	40.20%	58.30%
	6	10.40%	6.00%	15.00%	20.00%	31.00%	12.00%

conditions experienced at the study site (Chimner and Cooper, 2004; McLendon et al., 2008). Rainfall received in the study area from June 2015 till October 2016 was extremely low as shown in Fig. 7, with approximately 180 mm received during this period. However, a significant proportion of this rainfall was received from a single high magnitude event during March 2016, with only 73 mm being received prior to this event.

The rainfall received from this high magnitude event and the minor contributions from subsequent events, would have significantly increased soil water availability during the initial stages of the dry season, compared to the rest of study period (Riddell et al., 2017). Subsequently during May there was minimal ET_g; however, as the dry season progressed and aridity increased, there was an increase in GW uptake to fulfil a portion of the daily transpiration demand.

In addition to the seasonal changes in water uptake patterns, the species of riparian vegetation and their respective locations also showed variability in ET_g. Riparian vegetation situated along the southern bank of the study area generally used more GW to fulfil a portion of their transpiration demands, a trend which was consistent for each of the sampling campaigns. Whereas GW uptake by riparian vegetation situated within the river channel was consistently low.

Although GW represents a potential source to fulfil a portion of daily transpiration demands, especially as aridity increases, the accessibility of this resource for consumption and the amount used is largely controlled by the physiological characteristics of the plant/tree species (McLendon et al., 2008). In a similar environmental setting, February et al. (2007) showed that deep-rooted *P. violecia* were able to grow conservatively but consistently during conditions of water stress as they were able to access groundwater. Whereas the shallow rooted *C. mopane* predominantly relied upon available soil moisture and grew in rapid pulses in response to rainfall events.

These findings reaffirm our observations and provide further indication that individual tree species adopt alternative water use strategies to cope with conditions of water stress. Moreover, the depth to GW, as well as the physical properties of the soil and underlying aquifer may further influence the accessibility and use of this resource for plant water uptake (McLendon et al., 2008; Evaristo and McDonnell, 2017).

In order to quantify seasonal changes in GW use for the entire study area, all δ^2H and δ^{18}O values of xylem and source waters were respectively averaged for each sampling campaign. These values were then used as inputs to Simmr to determine source water contribution to transpiration. Spatial and seasonal variations in ET_g along the length of river reach studied was then determined as the product of these values (Table 4) and the satellite-derived ET pixel values covering the area of interest, as shown in Fig. 8. During May, the average ET_g for the entire study area was extremely low (0.01 mm d^{-1}), accounting for only 0.10% of daily ET. Whereas there was an increase in the average ET_g for August and October, with approximately 0.30 mm d^{-1} of GW being utilized during these months, as shown in Fig. 9.

Overall our results indicate that while GW use is prevalent and increases with aridity, the magnitude of ET_g is fairly minimal and lower than the global average (approximately 23%) reported in Evaristo and McDonnell (2017). Furthermore the results of the stable isotope analysis presented in Fig. 5 provides some evidence of ecohydrological separation (Evaristo et al., 2015) within our study site. δ^2H and δ^{18}O values for rainfall, stream water and GW from each of the sampling locations plot closely along the LMWL. However, δ^2H and δ^{18}O values for soil and xylem waters generally plot below these sources on the LMWL, signifying that the plant species within the study site are using soil water stores that are not contributing to streamflow or GW recharge (Evaristo et al., 2015).

Although the coupling of ET estimates from the satellite-based SEBS model with stable isotope analysis facilitated the quantification of seasonal and spatial variations in ET_g, the use of stable isotope analysis and a mixing model in this study may not necessarily provide an adequate insight on the actual plant water use dynamics within the study
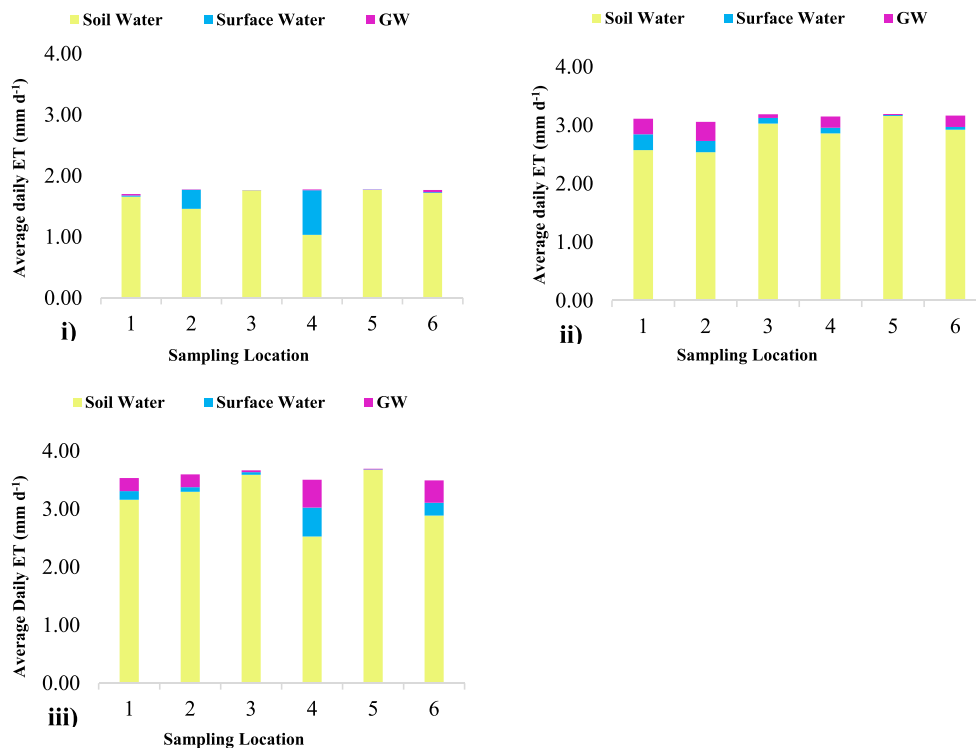
Fig. 6. Contribution of sources to ET (mm d^{-1}) at each sampling location during; i) May, ii) August and iii) October 2016.
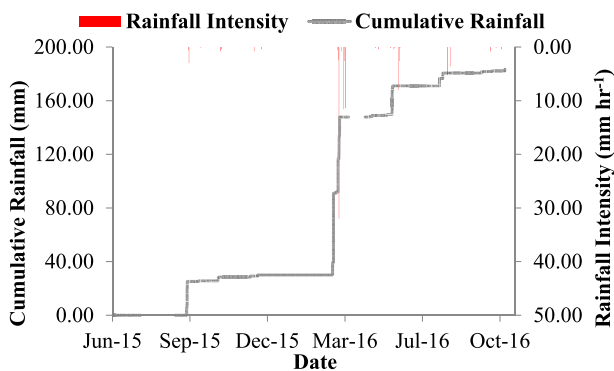

Fig. 7. Rainfall measured at Phalaubeni for the 2015/2016 hydrological year.

Table 4
Average proportional contribution of sources to ET for the study site during each sampling campaign.

Period (2016)	Ground water	Surface water	Soil water (30 cm)	Soil water (60 cm)	Soil water (100 cm)	Soil water (140 cm)
May (Late Autumn)	0.10%	0.10%	0.10%	0.10%	46.40%	53.10%
Aug (Mid-Winter)	10.00%	6.00%	12.00%	17.00%	38.40%	13.00%
Oct (Mid-Spring)	7.00%	6.20%	6.30%	7.00%	8.00%	63.00%

area, especially with regards to seasonal water use dynamics. This can be largely attributed to; i) the limited sampling frequency and number of samples collected for analysis and ii) general limitations and sources of uncertainty when using mixing models (Phillips et al., 2014). Furthermore, potentially significant differences in δ^{2}H composition between xylem and source waters due to isotopic fractionation during root water uptake may also lead to erroneous results, when using a single isotope ratio system (using δ^{2}H over δ^{18}O) in a mixing model (Zhao et al., 2016; Evaristo et al., 2017). However, Evaristo et al. (2017) notes that a Bayesian mixing model approach (such as Simmr) may be

insensitive to ^{2}H/^{1}H fractionation when using both δ^{2}H and δ^{18}O.

While the aforementioned limitations may hinder the feasibility of applying the methodology described herein to estimate ET_g, this approach is neither site or model specific. Therefore, these constraints may be addressed by; increasing the water sampling frequency and the number of water samples collected during various seasons, adhering to recommended guidelines for best practices in the use of stable isotope mixing models or implementing a satellite-based ET model which is able to better capture ET and energy fluxes in this particular environment.

5. Conclusion

The relative importance of GW as a resource to sustain terrestrial vegetation, especially during conditions of water stress has been well documented. However, understanding and accurately quantifying GW dependency by riparian vegetation in data scarce regions may prove to be challenging. For this purpose, we employed the satellite-based SEBS model to estimate ET. These estimates were coupled with stable isotope analysis to determine spatial and seasonal variations in GW use during transpiration. The results of these investigations showed that soil water was the main contributing source to ET. In general, GW use was prevalent within the study area, however, the magnitude of its contribution to transpiration was fairly minimal and not as significant as generally reported in literature.

While the integration of satellite-based ET estimates and stable isotope analyses enabled us to acquire estimates of seasonal and spatial variations in ET_g, it is important to take cognisance of the various limitations associated with this approach, as addressing these constraints will ultimately influence the accuracy of quantifying spatial and seasonal dynamics in ET_g, using the methodology adopted in this study.

Nevertheless, the coupling of the satellite-derived ET estimates with stable isotope analysis provides a relatively simplistic and inexpensive means of quantifying and spatially extrapolating, not only the contribution of GW to transpiration but soil and stream water as well. Such information can prove to be extremely useful in deriving seasonal and
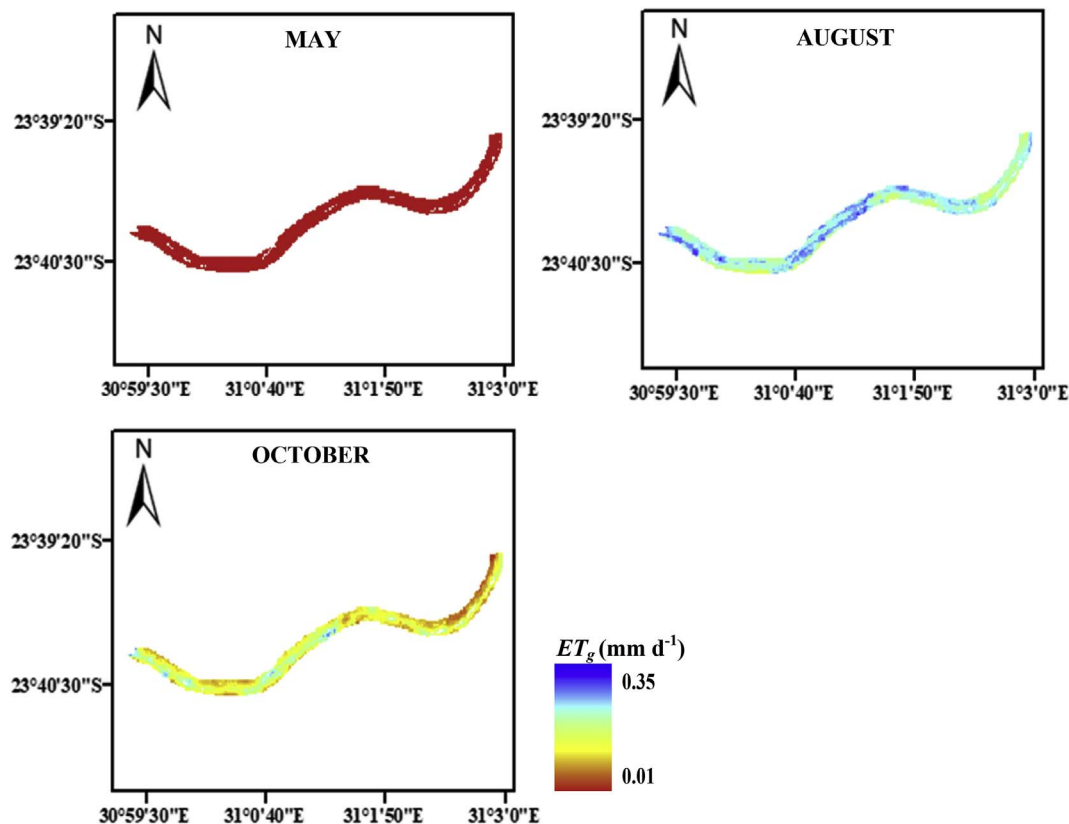
Fig. 8. A comparison of seasonal and spatial variations in *ETg* (mm d^{-1}) along the length of river reach studied.
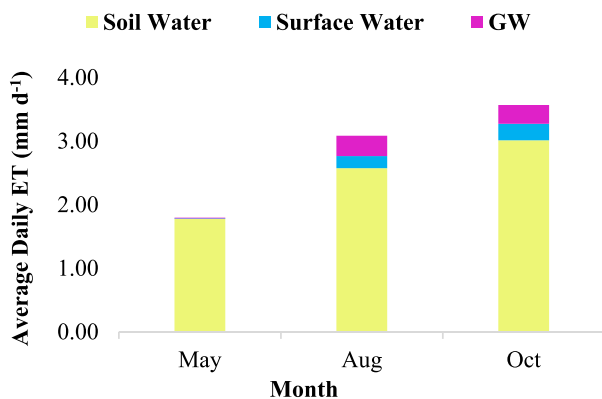

Fig. 9. A comparison of seasonal variations in the contribution of sources to ET during the three sampling campaigns.

spatially explicit water balances, which in turn can facilitate predicting how anthropogenic, climatic and environmental changes affect the rapport between plant growth and hydrological processes. This may prove particularly beneficial to inform water resources management decisions in data scarce regions, as it can be used to provide baseline estimates of seasonal and spatial GW dependency by riparian vegetation, facilitating the improved allocation of this resource for human and environmental requirements.

References

Allen, R.G., Pereira, L.S., Raes, D., Smith, M., 1998. Crop Evaporation: Guidelines for Computing Crop Water Requirements, FAO Irrigation and Drainage Paper No. 56. Food and Agriculture Organization of the United Nations, Rome, Italy92-5-104219-5.

Chimner, R.A., Cooper, D.J., 2004. Using stable oxygen isotopes to quantify the water source used for transpiration by native shrubs in the San Luis Valley, Colorado U.S.A. Plant Soil 260 (1–2), 225–236.

Craig, H., 1961. Isotopic variations in meteoric waters. Science 133, 1702–1703.

Daly, R.K., Tracy, R.S., Crout, N.M.J., Mairhofer, S., Pridmore, T.P., Mooney, S.J., Roose, T., 2017. Quantification of Root Water Uptake in Soil Using X-ray Computed Tomography and Image-based Modelling.

Dawson, T.E., Mambelli, S., Plamboeck, A.H., Templer, P.H., Tu, K.P., 2002. Annu. Rev. Ecol. Systemat. 2002 (33), 507–559.

Eamus, D., Zolfaghar, S., Villalobos-Vega, R., Cleverly, J., Huete, A., 2015. Groundwater-dependent ecosystems: recent insights from satellite and field-based studies. Hydrol. Earth Syst. Sci. 19, 4229–4256.

Ellsworth, P.Z., Williams, D.G., 2007. Hydrogen isotope fractionation during water uptake by woody xerophytes. Plant Soil. 291, 93–107.

Evaristo, J., McDonnell, J.J., 2017. Prevalence and magnitude of groundwater use by vegetation: a global stable isotope meta-analysis. Sci. Rep. 7, 44110.

Evaristo, J., McDonnell, J.J., Clemens, J., 2017. Plant source water apportionment using stable isotopes: a comparison of simple linear, two-compartment mixing model approaches. Hydrol. Process. 31, 3750–3758.

Evaristo, J., Jasechko, S., McDonnell, J.J., 2015. Global separation of plant transpiration from groundwater and streamflow. Nature 525, 91–94.

February, E.C., Higgins, S.I., Netwon, R., West, A.G., 2007. Tree distribution on a steep environmental gradient in an arid savanna. J. Biogeogr. 34, 270–278.

Fernández-Prieto, D., van Oevelen, P., Su, Z., Wagner, W., 2012. Advances in Earth

observation for water cycle science. Hydrol. Earth Syst. Sci. 16, 543–549.

Gibson, L.A., M̈unch, Z., Engelbrecht, J., 2011. Particular uncertainties encountered in using a pre-packaged SEBS model to derive evapotranspiration in a heterogeneous study area in South Africa. Hydrol. Earth Syst. Sci. 15, 295–310.

Gokool, S., Jarmain, C., Riddell, E., Swemmer, A., Lerm, R., Chetty, K.T., 2017a. Quantifying riparian total evaporation along the Groot Letaba River: a comparison between infilled and spatially downscaled satellite derived total evaporation estimates. J. Arid Environ. 147, 114–124.

Gokool, S., 2017b. Evaluating the Potential of Using Satellite Earth Observation Data to Quantify the Contribution of Riparian Total Evaporation to Streamflow Transmission Losses. Unpublished PhD Thesis. School of Agriculture Earth and Environmental Science, Centre for Water Resources Research, South Africa.

Heritage, G.L., Moon, B.P., Large, A.R.G., 2001. The February 2000 floods on the Letaba River, South Africa: an examination of magnitude and frequency. Koedoe 44 (2), 1–6.

Hong, S., Hendrickx, J.M.H., Borchers, B., 2011. Down-scaling of SEBAL derived evapotranspiration maps from MODIS (250 m) to Landsat (30 m) scales. Int. J. Rem. Sens. 32 (21), 6457–6477.

Jassas, H., Kanoua, W., Merkel, B., 2015. Actual evapotranspiration in the Al-Khazir gomal basin (northern Iraq) using the surface energy balance algorithm for land (SEBAL) and water balance. Geosciences 5, 141–159.

Katambara, Z., Ndiritu, J.G., 2010. A hybrid conceptual-fuzzy inference streamflow modelling for the Letaba River system in South Africa. Phys. Chem. Earth. 35 (13–14), 582–595.

Kogan, F., Guo, W., 2016. Strong 2015–2016 El Niño and implication to global ecosystems from space data. Int. J. Rem. Sens. 38 (1), 161–178.

Kumar, R., Shankar, V., Jat, M.K., 2014. Evaluation of root water uptake models–a review. ISH J. Hydraul. Eng. 21 (2), 115–124. http://dx.doi.org/10.1080/09715010.2014.981955.

Lange, J., 2005. Dynamics of transmission losses in a large arid stream channel. J. Hydrol. 306, 112–126.

Lin, G., da Sternberg, L.S.L., 1993. Hydrogen isotopic fractionation by plant roots during water uptake in coastal wetland plants. In: Ehleringer, J.R., Hall, A.E., Farquhar, G.D. (Eds.), Stable Isotopes and Plant Carbon-water Relations. Academic Press Inc, New York, pp. 497–510.

Lin, Z., Huili, Z., Xue, G., Yashu, Q.I., Xing, X., 2016. Seasonal patterns in water uptake for Medicago sativa grown along an elevation gradient with shallow groundwater table in Yanchi county of Ningxia, Northwest China. J. Arid Land. 8 (6), 921–934.

Liu, J.R., Song, X.F., Yuan, G.F., Sun, X.M., Yang, L.H., 2014. Stable isotopic compositions of precipitation in China. Tellus B 66, 22567.

Ma, Y., Song, X., 2016. Using stable isotopes to determine seasonal variations in water uptake of summer maize under different fertilization treatments. Sci. Total Environ. 550, 471–483.

Mares, R., Barnard, H.R., Mao, D., Revil, A., Singha, K., 2016. Examining diel patterns of soil and xylem moisture using electrical resistivity imaging. J. Hydrol. 536, 327–338.

Marwick, T.R., Tamooh, F., Teodoru, C.R., Borges, A.V., Darchambeau, F., Bouillon, S., 2015. The age of river-transported carbon: a global perspective. Global Biogeochem. Cycles 29, 122–137. http://dx.doi.org/10.1002/2014GB004911.

McLendon, T., Hubbard, P.J., Martin, D.W., 2008. Partitioning the use of precipitation- and groundwater-derived moisture by vegetation in an arid ecosystem in California. J. Arid Environ. 72, 986–1001.

Mekiso, F.A., Ochieng, G.M., Snyman, J., 2015. Isotope hydrology in the middle mohla-pitsi catchment, South Africa. Int. J. Eng. Res. Dev. 11 (01), 01–07.

Nippert, J.B., Knapp, A.K., 2007. Linking water uptake with rooting patterns in grassland species. Oecologia 153, 261–272.

Nourhi, H., Beecham, S., Kazemi, F., Hassanli, A.M., Anderson, S., 2013. Remote sensing techniques for predicting evapotranspiration from mixed vegetated surfaces. HESS Discuss 10, 3897–3925.

Penna, D., Oliviero, O., Assendelft, R., Zuecco, G., van Meerveld, I.H.J., Anfodillo, T., Carraro, V., Borga, M., Fontana, G.D., 2013. Tracing the water sources of trees and streams: isotopic analysis in a small pre-alpine catchment. Procedia Environ. Sci. 19, 106–112.

Pardo, N., Sanchez, L.M., Timmermans, J., Su, Z., Perez, I.A., Garcia, M.A., 2014. SEBS validation in a Spanish rotating crop. Agric. For. Meteorol. 195–196, 132–142.

Parnell, A., Inger, R., 2016. Stable isotope mixing Models in R with Simmr. https://cran.r-project.org/web/packages/simmr/simmr.pdf, Accessed date: 27 November 2016.

Phillips, D.L., Inger, R., Bearhop, S., Jackson, A.L., Moore, J.W., Parnell, A.C., Semmens, B.X., Ward, E.J., 2014. Best practices for use of stable isotope mixing models in food-web studies. Can. J. Zool. 92, 823–835.

Pollard, S., du Toit, D., 2011. Towards adaptive integrated water resources management in southern Africa: the role of self-organisation and multi-scale feedbacks for learning and responsiveness in the Letaba and crocodile catchments. Water Resour. Manag. 25 (15), 4019–4035.

Riddell, E.S., Nel, J.M., Gokool, S., Jarmain, C., Raubenheimer, R., Strydom, T., Swemmer, A., 2017. Quantification of transmission losses along the Letaba River for improved delivery of environmental water requirements (ecological reserve). Rep. Water Res. Comm Project Number K5/2338.

Riddell, E.S., Kilian, W., Versfeld, W., Kosoana, M., 2016. Groundwater stable isotope profile of the etosha national park, Namibia. Koedoe 58 (1), a1329. https://dx.doi.org/10.4102/koedoev58i1.1329.

Robinson, J.L., Slater, L.D., Schäfer, V.R., 2012. Evidence for spatial variability in hydraulic redistribution within an oak–pine forest from resistivity imaging. J. Hydrol. 430, 69–79.

Savage, M.J., Everson, C.S., Odhiambo, G.O., Mengistu, M.G., Jarmain, C., 2004. Theory and practice of evaporation measurement, with a special focus on SLS as an operational tool for the estimation of spatially-averaged evaporation. Rep. Water Res. Comm 1335/1/04, Pretoria, South Africa, 1-77005-247-X.

Schulze, R.E., Maharaj, M., Lynch, S.D., Howe, B.J., Melvil-Thomson, B., 1997. South African atlas of climatology and agrohydrology. Water Res. Comm Pretoria, Report TT82/96.

Singh, R.K., Senay, G.B., Velpuri, N.M., Bohms, S., Scott, R.L., Verdin, J.P., 2014. Actual evapotranspiration (water use) assessment of the Colorado river basin at the Landsat resolution using the operational simplified surface energy balance model. Rem. Sens. 6, 233–256.

Su, Z., 2002. The Surface Balance Energy System (SEBS) for estimating turbulent heat fluxes. Hydrol. Earth Syst. Sci. 6 (1), 85–99.

Su, Z., Wang, L., 2013. Earth Observation of Water Resources (SEBS). Practical Session Instructions (July 2013). ITC. University of Twente, The Netherlands.

Tanner, J.L., Hughes, D.A., 2015. Surface water–groundwater interactions in catchment scale water resources assessments: understanding and hypothesis testing with a hydrological model. Hydrol. Sci. J. 60 (11). http://dx.doi.org/10.1080/02626667.2015.1052453.

Thaw, M., Visser, A., Deinhart, A.L., Sharp, M., Everhart, A., Bibby, R.K., Conklin, M.H., 2016. Tracking water through the southern sierra critical zone observatory using radioactive and stable isotopes. In: Fall Meeting, American Geophysical Union, December 2016. Abstract H31K-07.

United States Geological Survey (USGS), 2015. Landsat 8 (l8) Data Users Handbook. Version 1.0. June 2015.

Villarreyes, C.A.R., Baroni, G., Oswald, S.E., 2013. Calibration approaches of cosmic-ray neutron sensing for soil moisture measurement in cropped fields. Hydrol. Earth Syst. Sci. 10, 4237–4274.

Walker, C., Richardson, S., 1991. The use of stable isotopes of water in characterizing the source of water in vegetation. Chem. Geol. 94 (2), 145–158.

West, A.G., Goldsmith, G.R., Matimati, I., Dawson, T.E., 2011. Spectral analysis software improves confidence in plant and soil water stable isotope analyses performed by isotope ratio infrared spectroscopy (IRIS). RCM (Rapid Commun. Mass Spectrom.) 25, 2268–2274.

White, J.W.C., Cook, E.R., Lawrence, J.R., Broecker, W.S., 1985. The D/H ratios of sap in trees: implications for watersources and tree ring D/H ratios. Geochem. Cosmochim. Acta 49 (1), 237–246.

Yang, Q., Xiao, H.L., Zhao, L.J., Zhou, M.X., Li, C.Z., Cao, S.K., 2010. Stable isotope techniques in plant water sources:a review. Sci. Cold. Arid Reg. 2 (2), 0112–0122.

Zimmermann, U., Münnich, K.O., Roether, W., Kreutz, W., Schubach, K., Siegel, O., 1966. Tracers determine movement of soil moisture and evapotranspiration. Science 152, 346–347.

Zhao, L., Wang, L., Cernusak, L.A., Liu, X., Xiao, H., Zhou, M., Zhang, S., 2016. Significant difference in hydrogen isotope composition between xylem and tissue water in Populus euphratica. Plant Cell Environ. 39 (8), 1848–1857.

Zhang, Z.Q., Evaristo, J., Li, Z., Si, B.C., McDonnell, J.J., 2017. Tritium analysis shows apple trees may be transpiring water several decades old. Hydrol. Process. 31, 1196–1201.